Attitude estimation and magnetometer calibration using reconfigurable TRIAD+filtering approach

Article *in* Aerospace Science and Technology · April 2020

DOI: 10.1016/j.ast.2020.105754

2 authors, including:

Halil Ersin Soken
Middle East Technical University
164 PUBLICATIONS **1,537** CITATIONS

SEE PROFILE

Attitude Estimation and Magnetometer Calibration Using Reconfigurable TRIAD+Filtering Approach

Halil Ersin Soken[1*] and Shin-ichiro Sakai[2]

[1] TUBITAK Space Technologies Research Institute, 06800 Çankaya, Ankara / TURKEY
e-mail: ersin.soken@tubitak.gov.tr

[2]Japan Aerospace Exploration Agency (JAXA), Institute of Space and Astronautical Science (ISAS) Yoshinodai 3-1-1, Chuo-ku, Sagamihara / JAPAN
e-mail: sakai@isas.jaxa.jp

* Corresponding Author

Abstract

This paper proposes using TRIAD and Unscented Kalman Filter (UKF) algorithms in a sequential architecture as a part of a small satellite attitude estimation algorithm. This TRIAD+UKF approach can both provide accurate attitude estimates for the satellite and calibrate the magnetometers in real-time. A complete calibration model for the magnetometers, considering bias, scale factor, soft iron and nonorthogonality errors, is assumed. In the algorithm's first stage, the TRIAD uses the available vector measurements (e.g. from Sun sensor and magnetometers) to estimate a coarse attitude. In the second stage, these estimated values are used as quaternion measurements in the UKF algorithm, together with the angular rate measured by a triad of gyros. The state vector for the UKF is composed of the attitude parameters, gyro biases and the magnetometer error terms. In result, we get

*Preprint submitted to Aerospace Science and Technology (*AESCTE) *August 30, 2019*
Published version can be accessed at https://doi.org/10.1016/j.ast.2020.105754

fine attitude estimate for the satellite by calibrating the magnetometers in real-time. Rather high computational load of the algorithm, mainly due to the additional states, is decreased by filter reconfiguration. We evaluate the algorithm for a hypothetical nanosatellite by numerical simulations. The results show that the attitude of the satellite can be estimated with accuracy better than 0.5deg and the magnetometers can be fully calibrated.

Keywords: attitude filtering; magnetometer calibration; small satellite; reconfigurable; TRIAD; UKF.

---

1. Introduction

Together with the increasing number of small satellite missions, attitude estimation for these satellites has become one of the popular research topics [1,2]. Apart from specific mission oriented discussions, we may say that the conducted researches try to answer two main questions: How to increase the attitude estimation accuracy, while using rather coarse attitude sensors because of the limitations [1,3,4]; and how to decrease the computational load of the algorithm so that it can be run even on a low-end microprocessor [5]? In this sense, it is important that the designed algorithm is capable of handling the sensor errors, most preferably in real time [6], and is computationally non-demanding.

One of these "rather coarse" attitude sensors for Low Earth Orbiting (LEO) small satellites is magnetometer [1,7–9]. Being lightweight, small, reliable and consuming low power are the main reasons for using this sensor in most of the small satellite missions. Yet, despite this popularity, magnetometers cannot provide very accurate attitude information due to several different errors corrupting the sensor measurements [10]. A proper real-time calibration algorithm is required when using the magnetometers for attitude estimation.

Published version can be accessed at https://doi.org/10.1016/j.ast.2020.105754

In line with the magnetometer's popularity as an attitude sensor, several different magnetometer calibration algorithms have been proposed. Examples vary widely in how the algorithm is designed. However, in any case, a magnetometer calibration algorithm that we can also use for small satellites must consider time-varying magnetometer errors (thus real-time applicable) [11,12]; and be computationally light for onboard implementation.

In [10], a detailed survey for calibration algorithms for small satellite magnetometers is done. In this study, among these presented algorithms, we are interested in attitude-dependent recursive algorithms. These algorithms require spacecraft attitude knowledge. There may be two sources for the attitude information: (1) the algorithm itself may estimate also the attitude [13]; (2) the attitude may be obtained from a sensor (e.g. star tracker) or a separate attitude estimator [14]. The magnetometers are calibrated using a recursive algorithm such as Kalman filter. Thus, even with a simple model, time variation for the error terms can be sensed.

In this study, we propose integrating the TRIAD algorithm with an unscented Kalman filter (UKF) to both estimate the attitude and calibrate the magnetometers. TRIAD and UKF work in a sequential architecture to form the overall algorithm. First the vector measurements from the magnetometers and Sun sensor are used in the TRIAD to estimate a coarse attitude. Then this coarse attitude information is fed into the UKF. The UKF uses the coarse attitude estimates by TRIAD and gyro readings as measurements for getting fine attitude estimates and further estimating the gyro biases and magnetometer error terms.

Integration of a single-frame attitude estimator with a type of Kalman filter was previously discussed for different single-frame estimators in different scenarios [15–19]. This is an advantageous approach for attitude filtering. Because, integrated algorithm has switching

flexibility between different sensors, without requiring dramatic modification in the filtering algorithm. Considering the limited hardware capability of small satellites and the vulnerability of small satellite sensors, such flexibility ensures sustainability of the mission for longer periods [20].

Compared to the existing literature, this paper proposes a complete magnetometer calibration model, which has not been discussed in any of previous publications mentioned above [15–19]. In a previous study, it is shown that a similar algorithm can be used for estimating the magnetometer biases together with the spacecraft's attitude, but the other error terms for magnetometers such as scaling were ignored [21]. In another study, a full calibration algorithm is proposed, but the algorithm is tested for a short duration without considering the eclipse [22]. In this paper we test our algorithm for an extended duration (for multiple orbit periods) considering also the eclipse. Moreover, we propose a reconfigurable version of the algorithm to decrease the rather high computational load, which is due to the additional states for magnetometer calibration. The reconfigurable filtering algorithm runs with the original configuration and estimates the magnetometer calibration parameters until the parameters converge to the steady state values. After the convergence, the filter estimates only the attitude parameters. In case any change is detected in the magnetometer error terms, the filter reconfigures back to the original algorithm to estimate the error terms again.

This paper continues with the mathematical model for satellite kinematics and sensors in Section II. Then in Section III we present the TRIAD+UKF algorithm for attitude estimation and complete magnetometer calibration. We discuss the filter reconfiguration to decrease the computational load also in this section. In Section IV, we demonstrate the algorithm's

Published version can be accessed at https://doi.org/10.1016/j.ast.2020.105754

performance with simulations for a hypothetical small satellite and test it in different scenarios.

2. Mathematical Models

2.1. Satellite Kinematics

When we use the quaternions for representing the satellite's attitude, the kinematics equation of motion can be given as [23],

$$\dot{\boldsymbol{q}}(t) = \frac{1}{2}\Omega(\boldsymbol{\omega}_{bi}(t))\boldsymbol{q}(t) \ . \tag{1}$$

Here $\boldsymbol{q}$ is the quaternion including four attitude parameters, $\boldsymbol{q} = \begin{bmatrix} q_1 & q_2 & q_3 & q_4 \end{bmatrix}^T$. Leading three variables represent the vector part and the last one is the scalar term. So we can rewrite the quaternion as $\boldsymbol{q} = \begin{bmatrix} \boldsymbol{g}^T & q_4 \end{bmatrix}^T$, where $\boldsymbol{g} = \begin{bmatrix} q_1 & q_2 & q_3 \end{bmatrix}^T$. Furthermore, in Eq. (1), $\Omega(\boldsymbol{\omega}_{bi})$ is the skew symmetric matrix as

$$\Omega(\boldsymbol{\omega}_{bi}) = \begin{bmatrix} 0 & \omega_z & -\omega_y & \omega_x \\ -\omega_z & 0 & \omega_x & \omega_y \\ \omega_y & -\omega_x & 0 & \omega_z \\ -\omega_x & -\omega_y & -\omega_z & 0 \end{bmatrix}, \tag{2}$$

where, $\boldsymbol{\omega}_{bi} = \begin{bmatrix} \omega_x & \omega_y & \omega_z \end{bmatrix}^T$ is angular velocity vector defining the body rates with respect to the Earth-centered inertial (ECI) frame.

The attitude matrix, A, can be given in terms of the quaternions as;

$$A = (q_4^2 - \boldsymbol{g}^2)I_{3\times 3} + 2\boldsymbol{g}\boldsymbol{g}^T - 2q_4\left[\boldsymbol{g}\times\right], \tag{3}$$

I_{3x3} is 3×3 identity matrix and $\left[\boldsymbol{g}\times\right]$ is the skew-symmetric matrix given as,

$$[\boldsymbol{g}\times]=\begin{bmatrix} 0 & -g_3 & g_2 \\ g_3 & 0 & -g_1 \\ -g_2 & g_1 & 0 \end{bmatrix}. \tag{4}$$

In the attitude filter, full quaternion vector with 4 components cannot be used, since the quaternion norm-constraint, given as $\boldsymbol{q}^T\boldsymbol{q}=1$, can be easily violated during the prediction phase. In literature there are several solutions proposed for this problem such as using Multiplicative and Additive versions of the Extended Kalman Filter (EKF) [23,24].

Problem solution, when UKF is used as the filtering algorithm, is similar. Instead of a four-component quaternion vector an unconstrained three-component vector is used to represent the attitude-error quaternion. In this paper, we use the Generalized Rodrigues Parameters (GRP) for representing the local error-quaternion following up the idea in [25].

First let us denote the local error-quaternion by $\delta\boldsymbol{q}=\begin{bmatrix}\delta\boldsymbol{g}^T & \delta q_4\end{bmatrix}^T$. Then the vector of GRP is

$$\delta\boldsymbol{p}=f\left[\delta\boldsymbol{g}/(a+\delta q_4)\right]. \tag{5}$$

In Eq.(5) scale factor f and tuning parameter a (a parameter from zero to one) are selected to decide how the local-error quaternion will be represented. If $a=0$ and $f=1$ Eq. (5) gives the Gibbs vector and if $a=1$ and $f=1$ it gives the standard vector of modified Rodrigues parameters. In line with the discussions in [25], we select $f=2(a+1)$. The inverse transformation from $\delta\boldsymbol{p}$ to $\delta\boldsymbol{q}$ is given by

$$\delta q_4=\frac{-a\|\delta\boldsymbol{p}\|^2+f\sqrt{f^2+(1-a^2)\|\delta\boldsymbol{p}\|^2}}{f^2+\|\delta\boldsymbol{p}\|^2}, \tag{6a}$$

$$\delta \boldsymbol{g} = f^{-1}(a + \delta q_4)\delta \boldsymbol{p} \ . \tag{6b}$$

2.2. Sensor Models

Gyros onboard the satellite, measure the body angular rate vector with respect to the ECI frame. The measurement model for gyros is

$$\tilde{\boldsymbol{\omega}}_{bi} = \boldsymbol{\omega}_{bi} + \boldsymbol{b}_g + \boldsymbol{\eta}_1, \tag{7}$$

where, $\tilde{\boldsymbol{\omega}}_{bi}$ is the measured angular rates of the satellite, $\boldsymbol{b}_g$ is the gyro bias vector as $\boldsymbol{b}_g = \begin{bmatrix} b_{gx} & b_{gy} & b_{gz} \end{bmatrix}^T$ and $\boldsymbol{\eta}_1$ is the zero mean Gaussian white noise with the characteristic of,

$$E\left[\boldsymbol{\eta}_{1k}\boldsymbol{\eta}_{1j}^T\right] = I_{3x3}\left(\sigma_v^2 / \Delta t\right)\delta_{kj}. \tag{8}$$

Here, σ_v is the gyro angular random walk value, δ_{kj} is the Kronecker symbol and Δt is the gyro sampling period. Gyro bias is modeled as a random walk process,

$$\dot{\boldsymbol{b}}_g = \boldsymbol{\eta}_2, \tag{9}$$

where $\boldsymbol{\eta}_2$ is also zero mean Gaussian white noise with the characteristic of,

$$E\left[\boldsymbol{\eta}_{2k}\boldsymbol{\eta}_{2j}^T\right] = I_{3x3}\left(\sigma_u^2 / \Delta t\right)\delta_{kj}. \tag{10}$$

Here, σ_u is the gyro rate random walk value.

The measurement equation for three-axis magnetometer (TAM) is [26],

$$\boldsymbol{B}_b = \left(I_{3\times3} + D\right)^{-1}\left(A\boldsymbol{B}_i + \boldsymbol{b}_m + \boldsymbol{\eta}_3\right), \tag{11}$$

where, $\boldsymbol{B}_b$ is the magnetometer measurements in the body frame, $\boldsymbol{B}_i$ is the reference magnetic field vector in the ECI frame, $\boldsymbol{b}_m = \begin{bmatrix} b_{mx} & b_{my} & b_{mz} \end{bmatrix}^T$ is the bias vector, D is the scaling matrix which reflects the scaling, symmetrical soft iron effects and nonorthogonality, and $\boldsymbol{\eta}_3$ is the zero mean Gaussian white noise with the characteristic of

$$E\left[\boldsymbol{\eta}_{3k}\boldsymbol{\eta}_{3j}^T\right] = I_{3x3}\sigma_m^2\delta_{kj}\,. \tag{12}$$

σ_m is the standard deviation of each magnetometer error.

Note that here we assume a symmetrical D matrix with six independent terms as

$$D = \begin{bmatrix} D_{11} & D_{12} & D_{13} \\ D_{12} & D_{22} & D_{23} \\ D_{13} & D_{23} & D_{33} \end{bmatrix}, \tag{13}$$

and neglect any non-symmetrical soft-iron errors and sensor misalignment. D matrix with nine independent components, accounting also for these errors, can be estimated without ambiguity only if we have an independent knowledge about attitude, such as the one from a star-tracker, or if we can apply a specific calibration maneuver [27].

The Earth magnetic field vector, $\boldsymbol{B}_i$, components in the ECI frame are calculated using the International Geomagnetic Reference Field (IGRF) model; 12th generation. Note that we model the measurements using the 10th order model, but the designed algorithm, which should be running onboard the satellite, is running with the 4th order model.

Sun direction model for calculating the direction vector in the ECI frame ($\boldsymbol{S}_i$) is rather easy and we need the exact Julian Day (T_{TDB}) for this model [15].

In the end we get the model for the Sun sensor measurements as,

$$\boldsymbol{S}_b = A\boldsymbol{S}_i + \boldsymbol{\eta}_4, \tag{14}$$

where, $\boldsymbol{S}_b$ is the vector for Sun sensor measurements in the body frame which are corrupted with, $\boldsymbol{\eta}_4$, the zero mean Gaussian white noise with the characteristic of

$$E\left[\boldsymbol{\eta}_{4k}\boldsymbol{\eta}_{4j}^T\right] = I_{3x3}\sigma_s^2\delta_{kj}\,. \tag{15}$$

σ_s is the standard deviation of Sun sensor error.

3. TRIAD+Filtering Approach for Attitude Estimation and Complete Magnetometer Calibration

3.1. Magnetometer Calibration Algorithm

In essence, the TRIAD+UKF is an algorithm designed for having accurate attitude estimates by incorporating all available information on attitude and calibrating the sensors. Despite using an accurate filtering algorithm within the overall architecture, it is aimed at keeping the computational load low by first processing the measurements in TRIAD and having a linear measurement moldel for the filter. The main reason of using TRIAD at the first stage is to show that the algorithm works well even with a simple single-frame estimator like TRIAD. In practice it may be replaced with more acclaimed algorithms such as QUEST. The TRIAD uses Sun sensor and magnetometer measurements to provide coarse attitude estimates. The UKF uses this coarse attitude information together with gyro measurements to give more accurate attitude estimations and estimate the additional parameters such as sensor error terms. The reason that we prefer using UKF rather than other attitude filtering algorithms such as EKF is mainly its capability to cope better with poor initialization. Due to the magnetometer error terms we have very coarse attitude information at the beginning

and the filter must be initialized with this poor state guess. The details for the sole TRIAD and UKF algorithms can be found in [21].

This TRIAD+UKF approach for attitude filtering and magnetometer calibration has two main advantages:

1) We can get only a coarse attitude estimate with the TRIAD algorithm, specifically at the beginning of the estimation process, when the UKF has not converged to the true magnetometer errors and the errors have not been compensated yet. Nonetheless, this attitude information from the TRIAD enables complete magnetometer calibration with a linear model.

Departing from the magnetometer measurement model (Eq.11), we can derive the measurement model for the recursive estimator in discrete time as,

$$A_k \boldsymbol{B}_{i,k} - \boldsymbol{B}_{b,k} = D_k \boldsymbol{B}_{b,k} - \boldsymbol{b}_{m,k} . \tag{16}$$

If it is reformulated

$$A_k \boldsymbol{B}_{i,k} - \boldsymbol{B}_{b,k} = \Phi_k \boldsymbol{\theta}_{m,k} , \tag{17}$$

where,

$$\boldsymbol{\theta}_m = \begin{bmatrix} \boldsymbol{b}_m^T & D_{11} & D_{22} & D_{33} & D_{12} & D_{13} & D_{23} \end{bmatrix}^T , \tag{18a}$$

$$\Phi = \begin{bmatrix} -1 & 0 & 0 & B_{bx} & 0 & 0 & B_{by} & B_{bz} & 0 \\ 0 & -1 & 0 & 0 & B_{by} & 0 & B_{bx} & 0 & B_{bz} \\ 0 & 0 & -1 & 0 & 0 & B_{bz} & 0 & B_{bx} & B_{by} \end{bmatrix} . \tag{18b}$$

Obviously, when the attitude is known, left hand side of Eq.17 are all known and the calibration problem can be easily solved with a linear Kalman filter (KF).

2) In the TRIAD+UKF approach the vector measurements are first processed with the TRIAD algorithm. The UKF uses the quaternion vector estimated by the TRIAD as measurements. Thus the measurement model for the attitude part of the filter is also linear. The measurement update phase for the UKF becomes same as the one for a linear Kaman filter. The linear measurement model decreases the computational demand more than 25% compared to the UKF which uses directly the vector measurements (in case we use the filter for only attitude estimation) [21]. Computational efficiency is even higher when compared to an UKF that estimates attitude and magnetometer error terms all together, with an augmented state approach (in this approach sole UKF uses the vector measurements and runs to estimate all the states including the magnetometer errors, simultaneously). Such computational saving is beneficial especially for nanosatellites with limited resources.

The scheme for the TRIAD+UKF algorithm for attitude estimation and magnetometer calibration is given in Fig.1. The TRIAD algorithm runs at the first stage using magnetometer ($\bar{\boldsymbol{B}}_b$) and Sun sensor ($\boldsymbol{S}_b$) measurements and estimates a coarse attitude ($\hat{\boldsymbol{q}}_{tr}$). The UKF in the second stage uses this coarse attitude information together with the angular rates from gyros ($\bar{\boldsymbol{\omega}}_{BI}$) as measurements. The UKF runs for estimating the state vector of

$$\boldsymbol{x} = \begin{bmatrix} \boldsymbol{q}^T & \boldsymbol{b}_g^T & \boldsymbol{\theta}_m^T \end{bmatrix}^T . \tag{19}$$

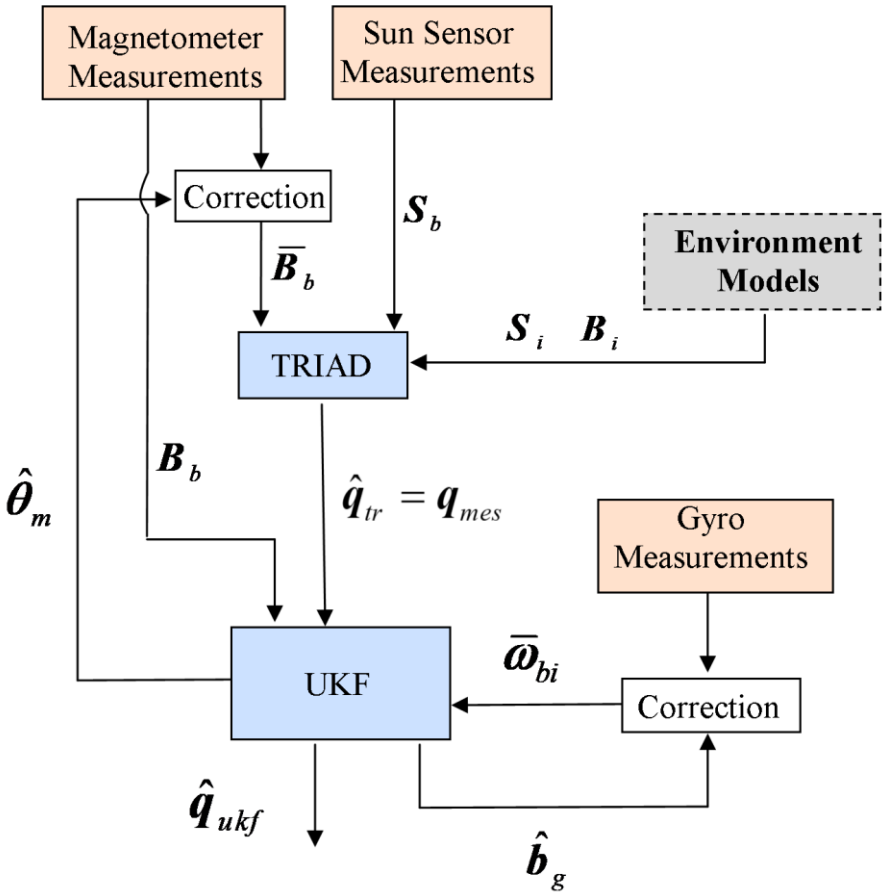

Fig. 1. TRIAD+UKF approach for attitude estimation and complete magnetometer calibration.

Note that here we use corrected TAM measurements in the TRIAD (represented as $\bar{\boldsymbol{B}}_b$ with an over bar), whereas the UKF still needs raw magnetometer measurements. The magnetometer measurements are corrected using the magnetometer error estimates of the UKF from the previous recursive step as

$$\bar{\boldsymbol{B}}_{b,k+1} = \left(I_{3\times 3} + \hat{D}_k\right)\boldsymbol{B}_{b,k+1} - \hat{\boldsymbol{b}}_{m,k}\,. \tag{20}$$

We need to apply a similar correction to the gyro measurements. The body angular rate vector with respect to the ECI frame ($\boldsymbol{\omega}_{bi}$) in Eq.(1) is replaced with the corrected gyro measurements. The measurements are corrected using the UKF gyro bias estimates from one previous recursive step,

$$\bar{\boldsymbol{\omega}}_{bi,k+1} = \tilde{\boldsymbol{\omega}}_{bi,k+1} - \hat{\boldsymbol{b}}_{g,k} . \tag{21}$$

Before using the TRIAD quaternion estimations as measurements in the UKF algorithm, the attitude error measurement in terms of GRP should be calculated,

$$\delta \boldsymbol{q}_{obs} = \boldsymbol{q}_{mes} \otimes \left[\hat{\boldsymbol{q}}_{0,k+1|k} \right]^{-1} . \tag{22}$$

Here, $\boldsymbol{q}_{mes}$, are the quaternion measurements from the TRIAD and quaternion-multiplied with the predicted mean quaternion, $\hat{\boldsymbol{q}}_{0,k+1|k}$. Then, in the light of $\delta \boldsymbol{q}_{obs} = \left[\delta \boldsymbol{g}_{obs}^{T} \quad \delta q_{4,obs} \right]^{T}$ equation, the attitude error measurement can be calculated as,

$$\delta \boldsymbol{p}_{obs} = f\left[\delta \boldsymbol{g}_{obs} / (a + \delta q_{4,obs}) \right]. \tag{23}$$

The UKF at the second stage of the algorithm uses the attitude error measurements from the TRIAD and the magnetometer measurements. That said the magnetometer measurements are only for magnetometer bias estimation not for the attitude estimation. The UKF measurement vector is

$$\boldsymbol{y} = \left[\delta \boldsymbol{p}_{obs}{}^{T} \quad \left(\hat{A}_{tr} \boldsymbol{B}_i - \boldsymbol{B}_b \right)^{T} \right]^{T} . \tag{24}$$

The measurement noise covariance matrix for the UKF is composed of two parts: R_q, covariance for the attitude measurements, and R_b, covariance for the magnetometer

measurements. In the proposed approach, the TRIAD estimation covariance is used as the measurement noise covariance for attitude measurements as $R_q = P_{tr}$. The covariance for the magnetometer measurements is tuned depending on the magnetometer characteristics.

As mentioned the UKF has a linear measurement model since we use the attitude error measurements. In this case, using the UKF equations for calculating the predicted observation vector, observation covariance matrix, and cross-correlation matrix are no more needed [21]. For a linear measurement model these equations simplify to those of a linear KF. Despite we have additional magnetometer error terms to estimate, such simplification reduces the computational load of the overall algorithm.

The first of these equations is the predicted measurement vector:

$$\hat{y}_{k+1|k} = H_{k+1}\hat{x}_{k+1|k}. \tag{25}$$

Here H is the measurement matrix given as

$$H = \begin{bmatrix} I_{3\times3} & 0_{3\times12} \\ 0_{3\times6} & \Phi_{3\times9} \end{bmatrix}. \tag{26}$$

Next, the observation covariance matrix is calculated as,

$$P_{yy,k+1|k} = H_{k+1}P_{k+1|k}H_{k+1}^T. \tag{27}$$

Last equation that is different than the regular UKF equations is the cross-covariance matrix:

$$P_{xy,k+1|k} = P_{k+1|k}H_{k+1}^T. \tag{28}$$

After that the rest of the equations are same as the update phase of the UKF algorithm [21].

3.2. Reconfiguration for Computational Load Minimization

As discussed having linear measurements and not requiring sigma point calculations at the update stage reduce the computational load of the proposed filtering algorithm. Yet, due to the additional 9 states in Eq.(19) for magnetometer calibration, there is need for 31 sigma point calculations in the prediction step of the filter (note that we need $2n+1$ sigma points for an n dimensional state vector in the regular UKF algorithm). Repeating these calculations at every prediction step, nonetheless, increases the computational load.

Thus, we propose reconfiguring the filter to the attitude filter configuration that runs for estimating only the attitude states when the magnetometer error terms converge to the steady-state values. The magnetometer measurements are corrected using the last available calibration parameter estimates, which are kept in the memory, and the algorithm estimates only the attitude and the gyro biases.

The scheme for the reconfigurable algorithm is given in Fig.2. Until the convergence of the magnetometer calibration parameters the algorithm runs with the original configuration. In this case, the switches I are closed and the only difference from the scheme given in Fig.1 is the stopping rule and memory blocks added to the flow. We check the magnetometer calibration terms for convergence using the following stopping rule [28]:

$$r_{\theta,k}^2 = \left(\hat{\boldsymbol{\theta}}_{m,k} - \hat{\boldsymbol{\theta}}_{m,k-1}\right)^T \bar{P}_{\Delta\theta,k}^{-1} \left(\hat{\boldsymbol{\theta}}_{m,k} - \hat{\boldsymbol{\theta}}_{m,k-1}\right) \leq \varepsilon_\theta . \tag{29}$$

Here, $\bar{P}_{\Delta\theta,k}^{-1}$ is the covariance matrix of the discrepancy between two successive error state estimates $\hat{\boldsymbol{\theta}}_{m,k}$ and $\hat{\boldsymbol{\theta}}_{m,k-1}$, and ε_θ is a predetermined small number.

From the KF theory we know that the estimations for $\hat{\boldsymbol{\theta}}_{m,k}$ has Gaussian distribution. Then the discrepancy $\hat{\boldsymbol{\theta}}_{m,k} - \hat{\boldsymbol{\theta}}_{m,k-1}$ also has a normal distribution, since it is a linear

combination of these two Gaussian random variables. Considering this fact, the statistic r_θ^2 has a χ^2 distribution with c degrees of freedom (c is the number calibration parameters), and the threshold values of r_θ^2 can be found by referring to the χ^2 tables for a given level of significance.

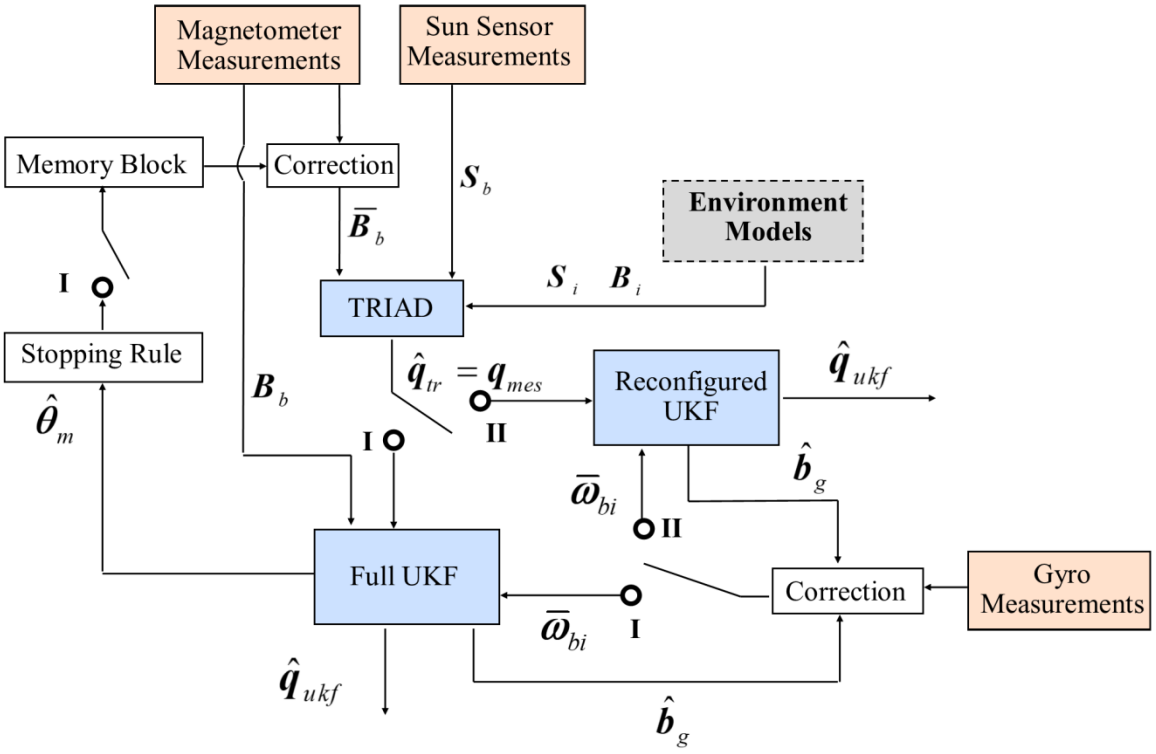

Fig. 2. Reconfigurable TRIAD+UKF approach for attitude estimation and complete magnetometer calibration.

Eq. (29) clearly shows that for smaller value of r_θ^2, the consistency of the estimates will be greater. Usually in the consistency tests in such cases, the lower limit of the confidence interval must be equal to zero, and the upper limit is determined by the level of significance α.

To test the consistency of the estimates, the level of significance α is adopted, which corresponds to the confidence coefficient $\beta = 1-\alpha$. The threshold $\chi^2_{\beta,c}$ is specified in terms of this probability, using the distribution of the investigated statistic r^2_θ:

$$P\left\{\chi^2 < \chi^2_{\beta,c}\right\} = \beta, \qquad 0 < \beta < 1. \tag{30}$$

The estimation process is stopped when $r^2_{\theta,k} < \chi^2_{\beta,c}$, since further parameter estimations yield insignificant improvement of the magnetometer calibration model. If the quadratic form r^2_θ is larger than, or equal to, the specified threshold $\chi^2_{\beta,c}$, estimation should be continued.

Once the inequality of $r^2_{\theta,k} < \chi^2_{\beta,c}$ is satisfied, the estimation of the magnetometer error terms is stopped and later on the magnetometer measurements are calibrated using the latest available parameter estimates which are kept in the memory. The filtering algorithm is reconfigured as an attitude filter (Attitude UKF) that estimates only the spacecraft's attitude and the gyro biases. In Fig.2, the switches I are open and the switches II are closed.

Regarding the covariance matrix of discrepancy between two successive error state estimates, $\bar{P}^{-1}_{\Delta\theta,k}$, based on the fact that the system model and the initial conditions (both for the state and the covariance's) are same for the estimated magnetometer error parameters, it can be shown that [28]:

$$\bar{P}_{\Delta\theta,k} = P_{\theta,k-1} - P_{\theta,k}. \tag{31}$$

Here $P_{\theta,k-1}$ and $P_{\theta,k}$ are covariance for the estimation of $\hat{\boldsymbol{\theta}}_m$ at two successive recursive steps. Note that the resulting $\bar{P}_{\Delta\theta,k}$ is a positive definite matrix.

Although, the reconfigured algorithm has reduced computational load, it is also incapable of sensing any change in the estimated calibration parameters. Once the estimation of the error terms is stopped, the algorithm assumes that the terms are same as the last saved ones in the memory block. In fact, the main reason for using a real-time calibration algorithm rather than the batch calibration of the magnetometer measurements is the possibility of change in errors for small satellite magnetometers under different circumstances. Onboard the small satellites the magnetometers are located close to the other subsystems because of size limitations. Thus, nearby electronics and magnetic torquers (MTQs), which are ideal actuators for attitude control of LEO small satellites [29], cause time-varying magnetometer errors [10–12].The reconfigured algorithm should sense any change in the magnetometer calibration parameters and reconfigure back to the original magnetometer calibration filter when the change is detected.

There are different methods available in literature to detect changes in the estimated parameters. In this study, the change is detected via a kind of statistical information. To do that we propose the following two hypothesis [30]:

- γ_o; there is no change in the system
- γ_1; the magnetometer calibration parameters have changed.

Then we may introduce the following statistical functions which is checked within the Attitude UKF,

$$\zeta_k = \boldsymbol{e}_k^T \left[P_{yy,k+1|k} + R_k \right]^{-1} \boldsymbol{e}_k . \tag{32}$$

Here, $\boldsymbol{e}_k = y_{k+1} - \hat{y}_{k+1|k}$ is the innovation vector. This function has χ^2 distribution with z degree of freedom, where z is the dimension of the innovation vector.

Next, as introduced in Eq.(30), we need to select a level of significance and corresponding confidence coefficient to determine a threshold value, $\chi^2_{\beta,z}$. Note that the selected α does not need to be same with the one selected for the stopping criteria.

In the end, when the hypothesis γ_1 is correct, the statistical value of ζ_k will be greater than the threshold value $\chi^2_{\beta,z}$, i.e.:

$$\begin{aligned} \gamma_0 &: \zeta_k \le \chi^2_{\beta,z} \qquad \forall k \\ \gamma_1 &: \zeta_k > \chi^2_{\beta,z} \qquad \exists k \quad . \end{aligned} \tag{33}$$

Thus, using ζ_k statistics we can detect if there is any change in the magnetometer calibration parameters. When the change is detected, the algorithm reconfigures to the original Magnetometer Calibration UKF and can be switched back to the attitude filter after the convergence of the filter to the new values of the calibration parameters.

4. Numerical Example

The proposed TRIAD+UKF approach for attitude filtering and complete magnetometer calibration is tested for a hypothetical LEO nanosatellite. On the ephemeris of this hypothetical nanosatellite the assumed values are $e = 6.4 \times 10^{-5}$ for the eccentricity, $i = 74^\circ$ for inclination and 612km for the (approximate) altitude.

The magnetometer noise is zero mean Gaussian white noise with a standard deviation of $\sigma_m = 300\text{nT}$. The assumed true values for the bias and scaling matrix terms are

$$\boldsymbol{b}_m = \begin{bmatrix} 5000 \\ 3000 \\ 4000 \end{bmatrix} \text{nT}; \qquad D = \begin{bmatrix} 0.05 & 0.05 & 0.05 \\ 0.05 & 0.1 & 0.05 \\ 0.05 & 0.05 & 0.05 \end{bmatrix}. \tag{34}$$

Moreover, the standard deviation for the Sun sensor noise is taken as $\sigma_s = 0.1^\circ$. It is assumed that the Sun sensor bias is negligible. For magnetometer and Sun sensor, the assumed noise levels are typical values for nanosatellite sensors [1]. The angular random walk and rate random walk values for the used gyros are $\sigma_v = 2.47 \text{ arcsec}/\sqrt{\text{s}}$ and $\sigma_u = 6.36 \times 10^{-4} \text{arcsec}/\sqrt{\text{s}^3}$, respectively.

The proposed algorithm is run for 6h, which is approximately six orbit periods for the satellite. The sampling time for all measurements is assumed to be $\Delta t = 1\text{s}$. We assume the spacecraft passes through the eclipse for approx. 1500s at every orbital revolution. Obviously, the Sun sensor measurements are not available in these periods.

Initial values for the UKF are set as $\hat{\boldsymbol{q}}_0 = \begin{bmatrix} 0 & 0 & 0 & 1 \end{bmatrix}^T$ for quaternions, $\hat{\boldsymbol{b}}_{g,0} = \boldsymbol{0}$ for gyro biases, $\hat{\boldsymbol{b}}_{m,0} = \begin{bmatrix} 2000 & 1000 & 1500 \end{bmatrix}^T \text{nT}$ for magnetometer biases and 0 for all $\hat{D}_0$ matrix components.

The process noise covariance matrix for the UKF is set as given below. The measurement noise covariance matrix is as described in Section III.

$$Q = \begin{bmatrix} 10^{-6} I_{3\times3} & 10^{-25} I_{3\times3} & 0_{3\times3} & 0_{3\times6} \\ 10^{-25} I_{3\times3} & 10^{-10} I_{3\times3} & 0_{3\times3} & 0_{3\times6} \\ 0_{3\times3} & 0_{3\times3} & 10 I_{3\times3} & 0_{3\times6} \\ 0_{6\times3} & 0_{6\times3} & 0_{6\times3} & 10^{-8} I_{6\times6} \end{bmatrix}. \quad (35)$$

4.1. Results for the Original Algorithm

Fig.3 presents the attitude estimation error for the TRIAD+UKF approach and the standalone TRIAD algorithm ($\hat{\boldsymbol{q}}_{ukf}$ and $\hat{\boldsymbol{q}}_{tr}$ in Fig.2, respectively). Shaded areas in the figure represent the eclipse. As seen the error converges below 0.5° at about 5000th s and this is an acceptable accuracy regarding the used sensors and their error characteristics. Almost periodic increases in the TRIAD estimation errors (e.g. at 9500th s.) are mainly due to the two measurement vectors approaching to parallelism. Before the convergence, the TRIAD+UKF attitude estimations are also affected by this phenomenon. Once the algorithm converges, this effect is mitigated in the TRIAD+UKF results by magnetometer error compensation and incorporating the gyro measurements (compare for example the estimation results at the 2nd daylight period – from 5000th s to 9500th s – and the last daylight period – from 29000th s to 33500th s).

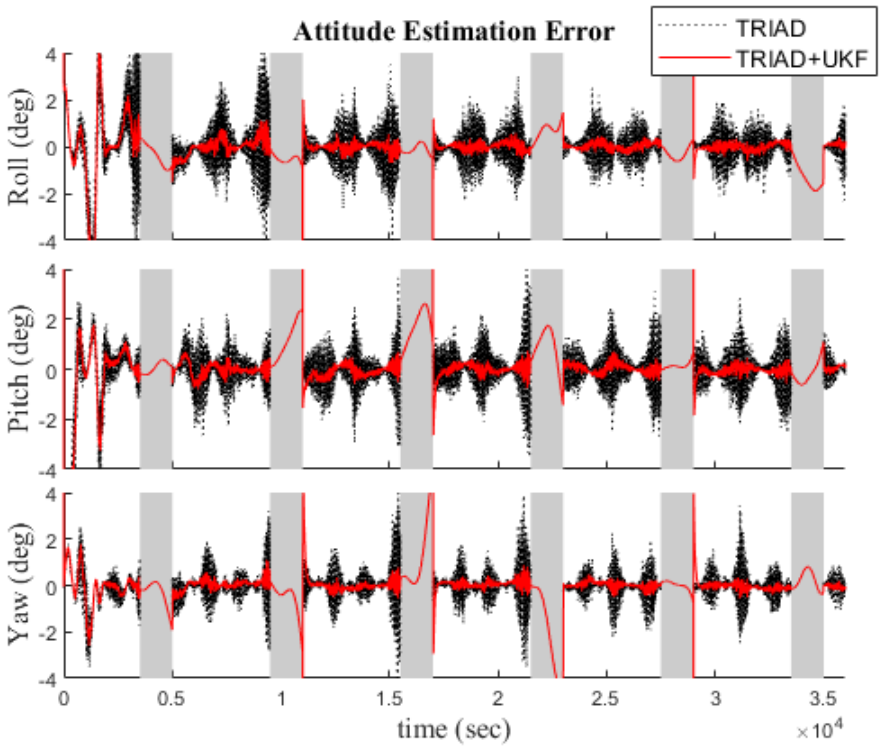

Fig. 3. Attitude estimation error for TRIAD and TRIAD+UKF algorithms. Presented TRIAD results are for the algorithm when it is run as a part of the proposed scheme.

Main issue with the attitude estimation results of the TRIAD+UKF algorithm is observed whenever the spacecraft passes through the eclipse and the eclipse ends. Because of having no measurements from the TRIAD, filter just propagates the attitude when the spacecraft is in eclipse. Inevitably, the estimation error increases in this period. Yet it hardly exceeds 5° and considering that the satellite is in eclipse and we do not have Sun sensor measurements it is an acceptable error, especially for small satellite missions. One obvious solution for filtering in eclipse might be using directly the vector measurements of the magnetometers, which are still available. However, since we do not want to change the main algorithm, we prefer just propagation without any measurement. Moreover, it should be kept in mind that,

if we use vector magnetometer measurements in the eclipse, we do not have a linear measurement model anymore and we need to repeat sigma point calculations at the update phase of the UKF, as well. This will considerably increase the computational load. Last but not least, in the absence of Sun sensor measurements, the proposed algorithm is not capable of estimating the magnetometer errors in eclipse. Considering that errors may change in eclipse periods due to the time-varying currents (mainly as a result of solar panel and battery duty cycles) [11], it can be concluded that for the proposed scheme just propagating the attitude in eclipses is more advantageous.

Fig. 4 gives the gyro bias estimation results in three axes. All components converge to the actual values rather quickly. At the eclipse-to-light transition the estimation error instantaneously increases. This is due to the filter's settings. Depending on the estimation covariance of the TRIAD, the measurement noise covariance for attitude measurements, R_q , changes at every recursive step. However, the process noise covariance matrix is kept fixed. Depending on the specific values of R_q , when the filter starts to receive the measurements, the filter may show an excited transient response until it converges again. We see that this is happening occasionally and after the 1st, 4th and 6th eclipse periods in the simulations (at about 6000th, 23000th and 35000th s, respectively) the filter has smoother responses. This can be avoided by increasing the process noise covariance for gyro bias terms, but of course doing so will also decrease the estimation accuracy in general. In any case because of the algorithm's configuration and using quaternion measurements from the TRIAD, these slight increases in the gyro bias estimates at the eclipse-to-light transitions do not affect the attitude estimation accuracy very much.

Figs. 5-7 present the estimation results for the magnetometer error terms. The filter quickly converges to the actual values, within two orbital periods. Convergence is rather slow for the D matrix terms, but for the magnetometer bias estimations, errors converge below 300nT (1σ) in approximately 3100th s.

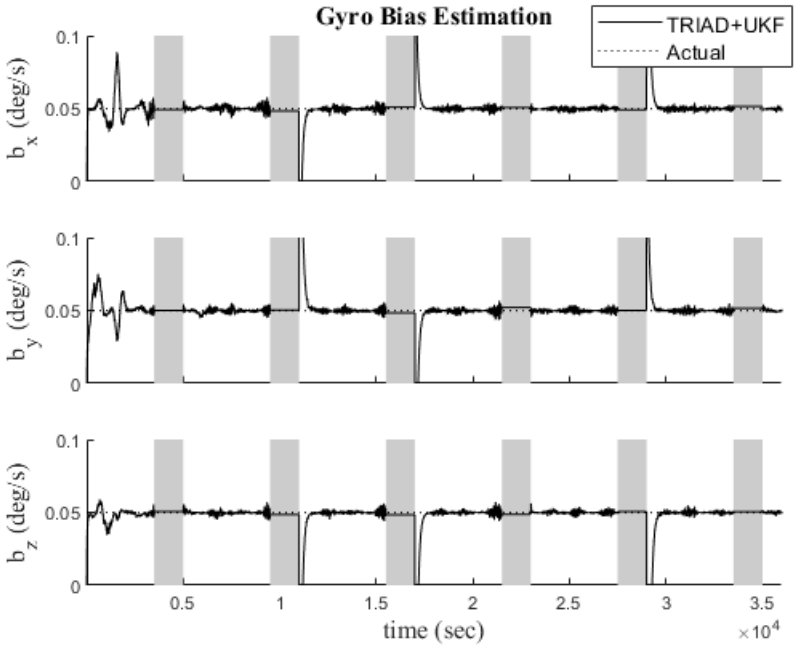

Fig. 4. Gyro bias estimation results for TRIAD+UKF algorithm.

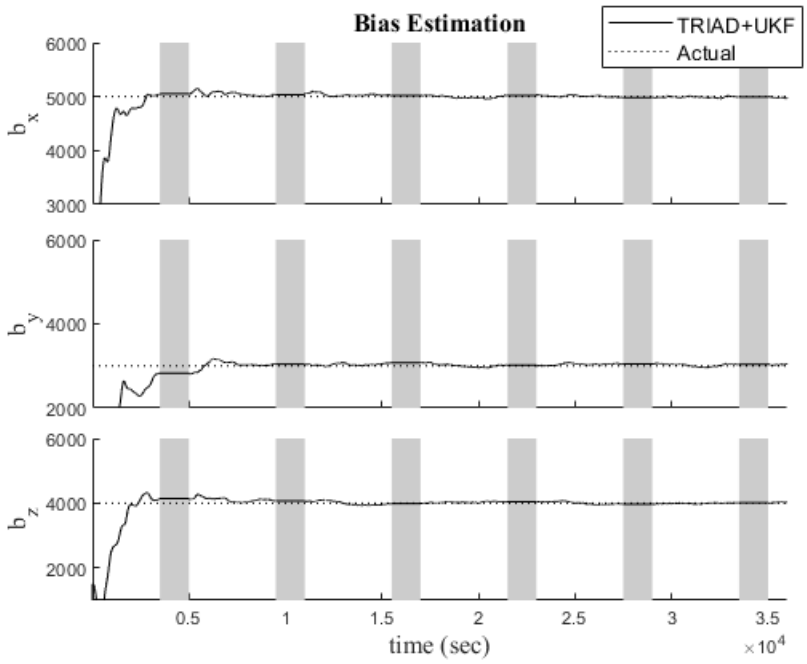

Fig. 5. Magnetometer bias estimation results for TRIAD+UKF algorithm.

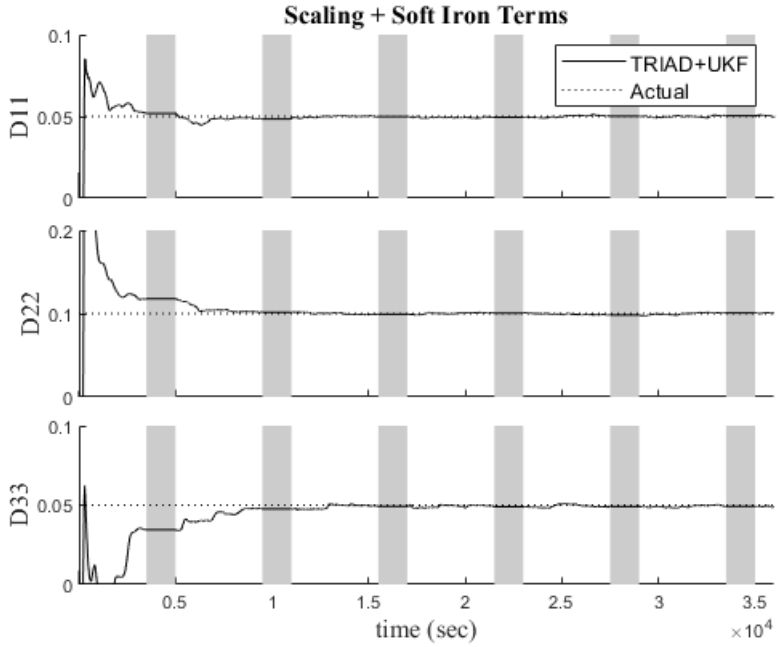

Fig. 6. Estimation results for the diagonal terms of the scaling matrix when TRIAD+UKF algorithm is used.

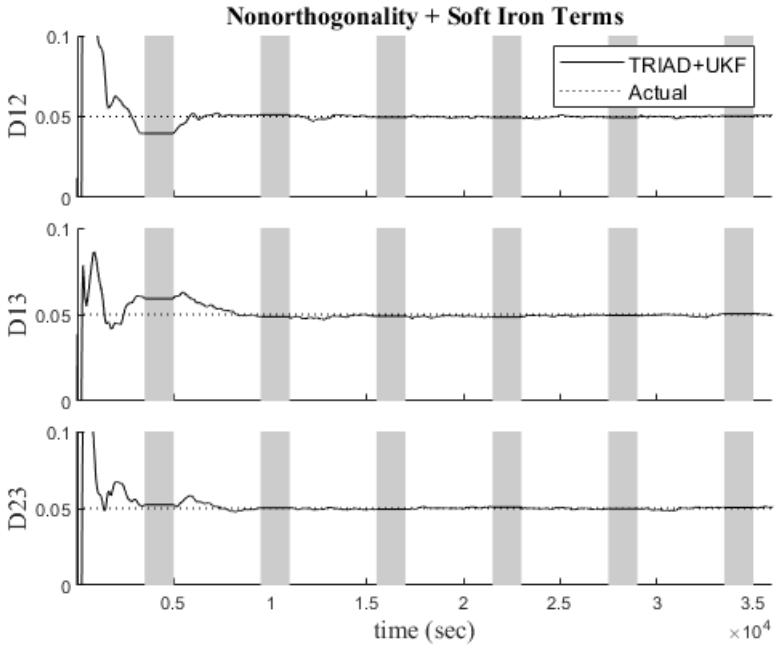

Fig. 7. Estimation results for the nondiagonal terms of the scaling matrix when TRIAD+UKF algorithm is used.

Overall, the proposed algorithm can estimate the attitude – in daytime – with an accuracy of 0.2313°, 0.2326° and 0.2026° (1σ) for roll, pitch and yaw angles, respectively and these values are far better than the desired accuracy of 1°. Filter achieves this accuracy level with successful real-time complete calibration of magnetometer errors.

Only drawback of the algorithm is the extended state size which is 15 including the magnetometer error terms. As discussed, in this case, we need to use 31 sigma points for calculations at the filter's prediction phase and this increases the computational load. Next section discusses the results for the reconfigured algoritm that we propose for reducing the computational load to a possible minimum level.

4.2. Results for the Reconfigured Algorithm

In this scenario, first the stopping rule, introduced with Eq. (29) is incorporated in the filtering algorithm and, when the criteria is met, the filter is reconfigured such that it uses the latest magnetometer estimation parameters kept in the memory and runs for estimating only the attitude and gyro biases (see Fig.2). Fig.8 presents the attitude estimation results for the algorithm for a representative run. To show the filter is running optimally, the attitude estimation error is given together with the $\pm 3\sigma$ bounds (blue lines). Scale is kept as in the original scenario for a fair comparison. After the reconfiguration (occurs approximately at 9000^{th} s and is represented with the dashed line) the estimation accuracy – in daytime - are 0.2327°, 0.2322° and 0.2027° (1σ) for roll, pitch and yaw angles, respectively. Compared to the original scenario with the Magnetometer Calibration UKF, the change is insignificant.

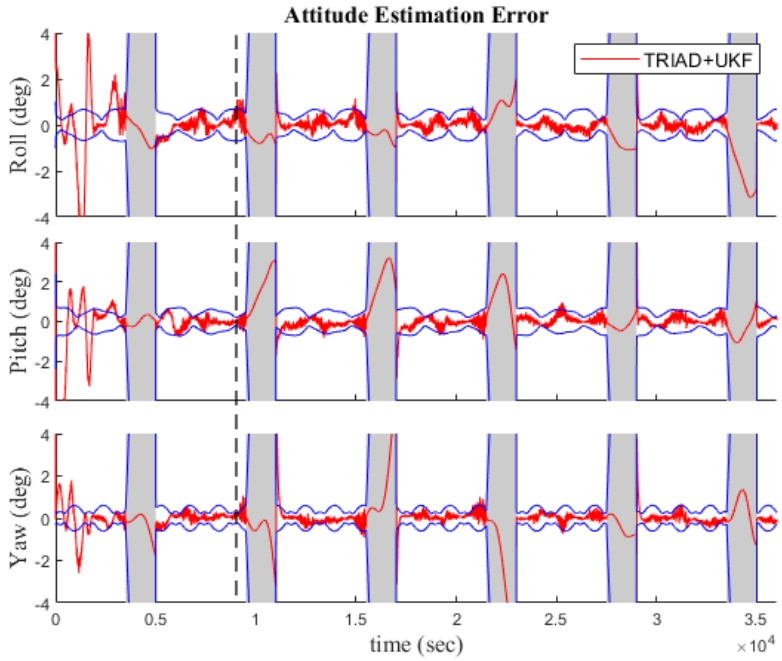

Fig. 8. Attitude estimation error for reconfigured TRIAD+UKF algorithm. Dashed line shows the approximate reconfiguration time.

Results show the filter maintains the same attitude estimation accuracy after the reconfiguration. Nonetheless, due to the reconfiguration, the computational load of the algorithm decreases 34.05%[1]. Note that this value reflects the mean value for 50 Monte Carlo runs and valid for this scenario which we compare the load when the filters run for 6h[2]. Obviously, in practice, when the filters run for the whole mission duration, this value will increase and using the reconfigurable algorithm will be more advantagous in terms of the computational load.

Although we save the computational resource, when the filter is reconfigured to the Attitude UKF, the algorithm becomes incapable of sensing any change in the magnetometer error terms. This is against our requirement for a real-time magnetometer calibration algorithm, which is necessary for small satellite missions [10]–[12]. Thus, as a second step we incorporate also the change detection test in the Attitude UKF and test the reconfigurable algorithm when a set of the magnetometer error parameters change.

Real mission experiences show that dramatic change in the magnetometer biases is more likely than a change in the *D* matrix elements [11], [12]. Change in the magnetometer bias terms is simulated as

$$\boldsymbol{b}_m = \begin{cases} \begin{bmatrix} 5000 & 3000 & 4000 \end{bmatrix} \text{nT} & t < 24000\text{s} \\ \begin{bmatrix} 4000 & 5000 & 2000 \end{bmatrix} \text{nT} & t \geq 24000\text{s} \end{cases} . \tag{37}$$

First of all, Fig.9 presents a section of ζ_k statistics just before the change in the magnetometer bias terms. As seen the statistics immediately exceeds the threshold, which is

[1]For reference, a representative run for the 10h long simulation scenario takes 23.5s for the original algorithm when the simulations are run on an Intel® Core™ i7-6700 CPU @ 3.40GHz and with a 32.0 GB RAM.
[2]Since the given value is the ratio it will be more or less same on any processor.

set as 11.34 for a level of significance of $\alpha = 0.01$. Hence the algorithm reconfigures back to the Magnetometer Calibration UKF for estimating the new level of biases. Note that the statistics is zero before 23000th s since the satellite is in eclipse and it is not calculated.

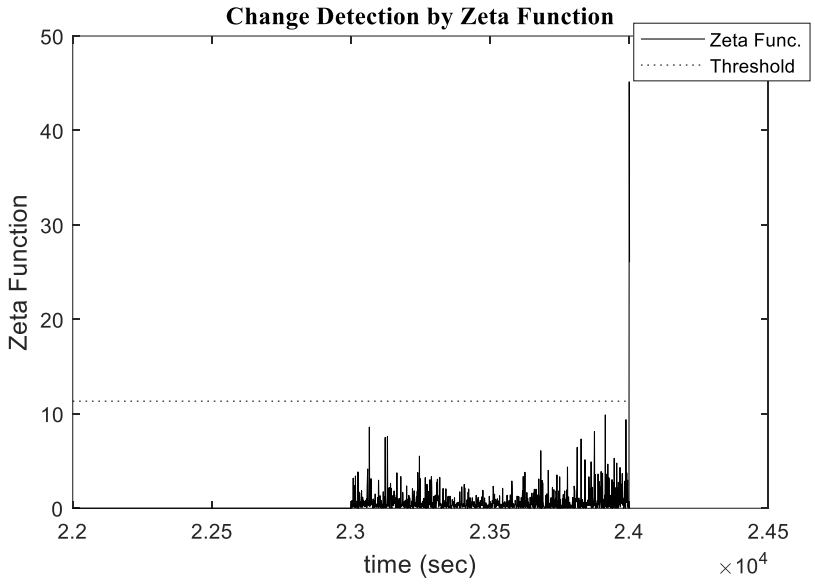

Fig. 9. Change detection using zeta function when the magnetometer biases change at 24000th s.

Fig. 10 gives the attitude estimation error for the reconfigured algorithm. Until 24000th s the results are similar to those presented in Fig.8. At 24000th s the magnetometer bias values change. After that the attitude estimation results deteriorates for few degrees for a period of approximately 2000s until the reconfigured filter converges to the new values of the magnetometer bias terms. Fig. 11 shows the magnetometer bias estimation results for the reconfigured filter. The filter responds to the change quickly – despite having a change that is rather large in magnitude – and converges to the actual values at about 27200th s (this instant is when the stopping rule in Eq.29 is satisfied; otherwise, as indicated, the attitude estimation errors fall into the $\pm 3\sigma$ bounds quicker, approximately 2000s after the change in

the magnetometer bias terms). Once the magnetometer bias estimations converge, the algorithm reconfigures back to the attitude filter that is estimating only the attitude and the gyro biases at about 27200th s.

Even in this scenario, where the algorithm needs to reconfigure to the Magnetometer Calibration UKF for an additional 3200s, the computational load is about 32.7% lesser compared to the original algorithm that estimates the magnetometer error terms all the time. That proves, whereever the magnetometer error term estimation is not needed, running the algorithm with the Attitude UKF saves considerable amount of computational resource.

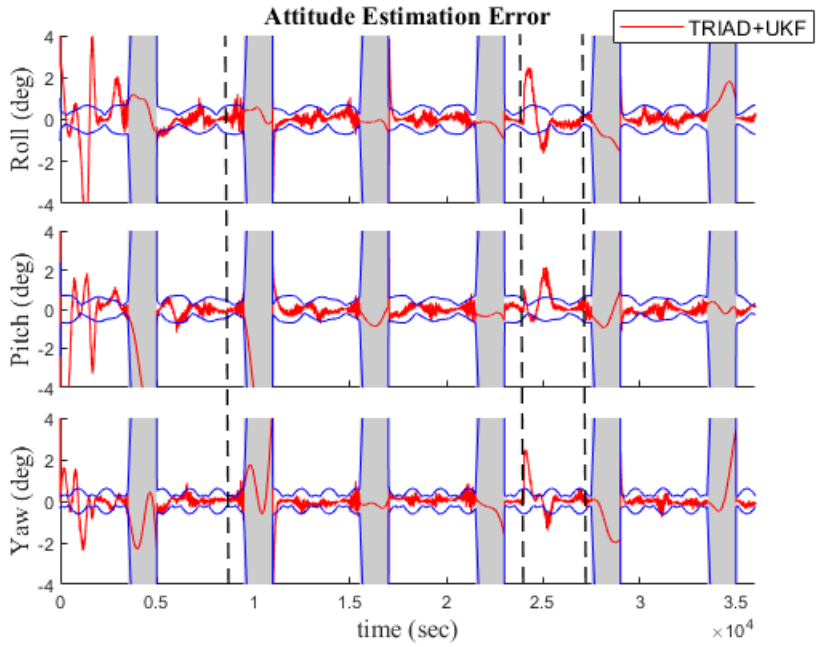

Fig. 10. Attitude estimation error for reconfigured TRIAD+UKF algorithm when magnetometer bias terms change at 24000th s. Dashed lines show the approximate reconfiguration times.

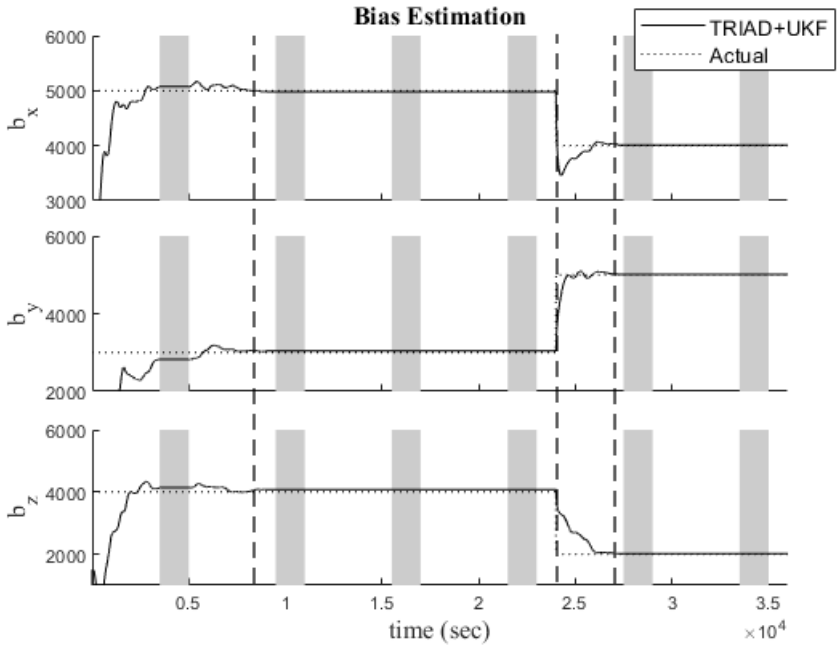

Fig. 11. Magnetometer bias estimation results for reconfigured TRIAD+UKF algorithm when magnetometer bias terms change at 24000th s.

4.3. Difficulties and Suggested Solutions

4.3.1. Tuning the Filter

In the proposed TRIAD+UKF approach it is assumed that the measurement noise for the UKF stage is uncorrelated, Gaussian white noise. However, in fact, there is correlation in between the noise covariance for the attitude measurements, R_q , and the magnetometer measurements R_b , since we use the same magnetometer measurements for attitude estimation in TRIAD. This correlation makes tuning the *R* matrix difficult (and actually this is another reason why we use UKF, which is more capable of coping with non-Gaussian noise compared to the EKF). Specifically, setting R_b part depending on the exact

magnetometer noise characteristics does not give the best estimation performance in terms of accuracy and convergence time.

On the process noise covariance matrix, Q, we have a 15×15 covariance matrix that should be tuned for optimal filter performance in the Magnetometer Calibration UKF configuration. Ratio of each Q term with respect to the R matrix terms must be considered as well, for such heuristic tuning process. As discussed, R_q values, which are changing at every recursive step depending on the accuracy of the TRIAD estimates, makes such tuning process even more challenging.

Considering the correlation in between the measurements for the UKF as well as difficult tuning process for both R and Q matrices, a possible solution might be using an adaptive version of the UKF [31]. An adaptive UKF algorithm may improve both the accuracy and the convergence rate.

4.3.2. Accuracy and stability issues due to frequent changes in the magnetometer error terms:

In this study, we assume that the magnetometer error terms do not change frequently. In practice, related to the mission characteristics and the satellite configuration, magnetometer error terms may change frequently. It happens due to the actuation of the magnetic torquers and/or change in the current in the circuits whenever the satellite is in/out of the eclipse. In case of frequent changes, the filter needs to reconfigure itself several times and, as observed in Fig.10, depending on also the magnitude of the change, such changes temporarily

deteriorates the filter's attitude estimation accuracy until the filter settles to the new values of the magnetometer error terms. Frequent changes may even affect the algorithm's stability.

Certainly, in case of frequent changes that are also large in magnitude, the rational way of implementation would be running the algorithm with the original scheme in Fig.1 and estimating the magnetometer error terms all the time without reconfiguring the filter. Although, we sacrifice the computational resource, we will ensure the filter's stability and the accuracy by doing so.

4. Conclusions

This paper proposes using TRIAD and Unscented Kalman Filter (UKF) algorithms in a sequential architecture to estimate the attitude and calibrate the magnetometers of a small satellite. In algorithm's first stage, the TRIAD uses the available vector measurements to estimate a coarse attitude. In the second stage, these estimated values are used as quaternion measurements in the UKF algorithm, together with angular rate measurements provided by a triad of gyros. The UKF state vector is composed of the attitude, gyro biases and the magnetometer error terms. In result, we get fine attitude estimates for the satellite and can calibrate the magnetometers against scaling, soft iron, nonorthogonality and bias errors in real time.

A reconfigurable algorithm is further proposed to decrease the rather high computational load of the algorithm which is mainly due to the additional magnetometer error states. The reconfigurable algorithm runs with a Magnetometer Calibration UKF only if necessary and for all other times it runs with the Attitude UKF that estimates only the attitude parameters

and the gyro biases. Algorithm reconfiguration times are detected by the proposed stopping and change detection rules.

The main contribution of this research is having a computationally light algorithm that is capable of providing accurate attitude estimates by calibrating the magnetometers in real-time. The demonstrations for a nanosatellite prove the capability of the algorithm for both attitude estimation and complete magnetometer calibration. Results show that the algorithm can provide an attitude estimation accuracy higher than 0.5°, which is sufficient for most of the nanosatellite applications. Further investigations will aim on testing the algorithm on an actual mission.

References

[1] D. Ivanov, M. Ovchinnikov, N. Ivlev, S. Karpenko, Analytical study of microsatellite attitude determination algorithms, Acta Astronaut. 116 (2015) 339–348. doi:10.1016/j.actaastro.2015.07.001.

[2] L. Cao, D. Qiao, X. Chen, Laplace ℓ1 Huber based cubature Kalman filter for attitude estimation of small satellite, Acta Astronaut. 148 (2018) 48–56. doi:10.1016/j.actaastro.2018.04.020.

[3] M. Kiani, Robust integrated orbit and attitude estimation using geophysical data, Aerosp. Sci. Technol. 93 (2019) 105307. doi:10.1016/j.ast.2019.105307.

[4] D. Cilden-Guler, M. Raitoharju, R. Piche, C. Hajiyev, Nanosatellite attitude estimation using Kalman-type filters with non-Gaussian noise, Aerosp. Sci. Technol. 92 (2019) 66–76. doi:10.1016/j.ast.2019.05.055.

[5] P. Zagorski, T. Dziwinski, A. Tutaj, Steepest descent quaternion attitude estimator,

Aerosp. Sci. Technol. 77 (2018) 1–10. doi:10.1016/j.ast.2018.01.030.

[6] J.C. Springmann, A.J. Sloboda, A.T. Klesh, M.W. Bennett, J.W. Cutler, The attitude determination system of the RAX satellite, Acta Astronaut. 75 (2012) 120–135. doi:10.1016/j.actaastro.2012.02.001.

[7] J.C. Springmann, J.W. Cutler, Flight results of a low-cost attitude determination system, Acta Astronaut. 99 (2014) 201–214. doi:10.1016/j.actaastro.2014.02.026.

[8] S. Nakasuka, K. Miyata, Y. Tsuruda, Y. Aoyanagi, T. Matsumoto, Discussions on attitude determination and control system for micro/nano/pico-satellites considering survivability based on Hodoyoshi-3 and 4 experiences, Acta Astronaut. 145 (2018) 515–527. doi:10.1016/j.actaastro.2018.02.006.

[9] A. Slavinskis, H. Ehrpais, Kuuste H, I. Sünter, J. Viru, J. Kütt, E. Kulu, M. Noorma, Flight Results of ESTCube-1 Attitude Determination System, J. Aerosp. Eng. 29 (2015) 4015014–4015017. doi:10.1061/(ASCE)AS.1943-5525.0000504.

[10] H.E. Soken, A survey of calibration algorithms for small satellite magnetometers, Meas. J. Int. Meas. Confed. 122 (2018) 417–423. doi:10.1016/j.measurement.2017.10.017.

[11] J.C. Springmann, J.W. Cutler, Attitude-Independent Magnetometer Calibration with Time-Varying Bias, J. Guid. Control. Dyn. 35 (2012) 1080–1088. doi:10.2514/1.56726.

[12] E. Kim, H. Bang, S.-H. Lee, Attitude Independent Magnetometer Calibration Considering Magnetic Torquer Coupling Effect, J. Spacecr. Rockets. 48 (2011) 691–694. doi:10.2514/1.52634.

[13] T. Inamori, N. Sako, S. Nakasuka, Strategy of magnetometer calibration for nano-satellite missions and in-orbit performance, in: AIAA Guid. Navig. Control Conf., American Institute of Aeronautics and Astronautics, Toronto, 2010. doi:10.2514/6.2010-7598.

[14] Y. Cheng, J.L. Crassidis, An expectation-maximization approach to attitude sensor calibration, Adv. Astronaut. Sci. 130 PART 2 (2008) 1749–1764.

[15] D. Cilden, H.E. Soken, C. Hajiyev, Nanosatellite attitude estimation from vector measurements using SVD-AIDED UKF algorithm, Metrol. Meas. Syst. 24 (2017). doi:10.1515/mms-2017-0011.

[16] D. Cilden, C. Hajiyev, H.E. Soken, Attitude and attitude rate estimation for a nanosatellite using SVD and UKF, in: RAST 2015 - Proc. 7th Int. Conf. Recent Adv. Sp. Technol., 2015. doi:10.1109/RAST.2015.7208431.

[17] C. Hajiyev, M. Bahar, Attitude determination and control system design of the ITU-UUBF LEO1 satellite, Acta Astronaut. 52 (2003) 493–499. doi:http://dx.doi.org/10.1016/S0094-5765(02)00192-3.

[18] Y. Nakajima, N. Murakami, T. Ohtani, Y. Nakamura, K. Hirako, K. Inoue, SDS-4 Attitude Control System: In-Flight Results of Three Axis Attitude Control for Small Satellites, in: 19th IFAC Symp. Autom. Control Aerosp., IFAC, 2013: pp. 283–288. doi:http://dx.doi.org/10.3182/20130902-5-DE-2040.00077.

[19] S. Esteban, J.M. Girón-Sierra, Ó.R. Polo, M. Angulo, Signal conditioning for the kalman filter: Application to satellite attitude estimation with magnetometer and sun sensors, Sensors (Switzerland). 16 (2016). doi:10.3390/s16111817.

[20] D.Y. Lee, H. Park, M. Romano, J. Cutler, Development and experimental validation of a multi-algorithmic hybrid attitude determination and control system for a small satellite, Aerosp. Sci. Technol. 78 (2018) 494–509. doi:10.1016/j.ast.2018.04.040.

[21] H.E. Söken, An Attitude Filtering and Magnetometer Calibration Approach for Nanosatellites, Int. J. Aeronaut. Sp. Sci. 19 (2018) 164–171. doi:10.1007/s42405-018-0020-8.

[22] H.E. Soken, S. Sakai, TRIAD+Filtering Approach for Complete Magnetometer Calibration, in: 2019 9th Int. Conf. Recent Adv. Sp. Technol., 2019: pp. 703–708. doi:10.1109/RAST.2019.8767427.

[23] F.L. Markley, J.L. Crassidis, Fundamentals of Spacecraft Attitude Determination and Control, Springer New York, New York, NY, 2014. doi:10.1007/978-1-4939-0802-8.

[24] V. Pesce, M.F. Haydar, M. Lavagna, M. Lovera, Comparison of filtering techniques for relative attitude estimation of uncooperative space objects, Aerosp. Sci. Technol. 84 (2019) 318–328. doi:10.1016/j.ast.2018.10.031.

[25] J. Crassidis, F.L. Markley, Unscented Filtering for Spacecraft Attitude Estimation, J. Guid. Control. Dyn. 26 (2003) 536–542. doi:10.2514/2.5102.

[26] H.E. Soken, A survey of calibration algorithms for small satellite magnetometers, in: 2017 IEEE Int. Work. Metrol. Aerosp., IEEE, 2017: pp. 62–67. doi:10.1109/MetroAeroSpace.2017.7999539.

[27] B.A. Riwanto, T. Tikka, A. Kestila, J. Praks, Particle Swarm Optimization with Rotation Axis Fitting for Magnetometer Calibration, IEEE Trans. Aerosp. Electron.

Syst. 9251 (2017) 1–1. doi:10.1109/TAES.2017.2667458.

[28] H.E. Soken, C. Hajiyev, UKF-based reconfigurable attitude parameters estimation and magnetometer calibration, IEEE Trans. Aerosp. Electron. Syst. 48 (2012) 2614–2627. doi:10.1109/TAES.2012.6237612.

[29] A. Sofyalı, E.M. Jafarov, R. Wisniewski, Robust and global attitude stabilization of magnetically actuated spacecraft through sliding mode, Aerosp. Sci. Technol. 76 (2018) 91–104. doi:10.1016/j.ast.2018.01.022.

[30] H.E. Soken, C. Hajiyev, S.-I. Sakai, Robust Kalman filtering for small satellite attitude estimation in the presence of measurement faults, Eur. J. Control. 20 (2014). doi:10.1016/j.ejcon.2013.12.002.

[31] H.E. Soken, UKF Adaptation and Filter Integration for Attitude Determination and Control of Nanosatellites with Magnetic Sensors and Actuators, The Graduate University for Advanced Studies, 2013. https://ir.soken.ac.jp/?action=pages_view_main&active_action=repository_view_main_item_detail&item_id=4899&item_no=1&page_id=29&block_id=155.